

Coexistence of color superconductivity and chiral symmetry breaking within the NJL model

D.Blaschke^{1,2}, M.K.Volkov², and V.L.Yudichev²

¹)*Fachbereich Physik, Universität Rostock, D-18051 Rostock, Germany*

²)*Joint Institute for Nuclear Research, 141980 Dubna, Russian Federation*

Abstract

The phase diagram for quark matter is investigated within a simple Nambu–Jona-Lasinio model without vector correlations. It is found that the phase structure in the temperature–density plane depends sensitively on the parametrization of the model. We present two schemes of parametrization of the model where within the first one a first order phase transition from a phase with broken chiral symmetry to a color superconducting phase for temperatures below the triple point at $T_t = 55$ MeV occurs whereas for the second one a second order phase transition for temperatures below $T_t = 7$ MeV is found. In the latter case, there is also a coexistence phase of broken chiral symmetry with color superconductivity, which is a new finding within this class of models. Possible consequences for the phenomenology of the QCD phase transition at high baryon densities are discussed.

Rostock University
Preprint No. MPG-VT-UR 235/02

1 Introduction

The phenomenon of color superconductivity [1, 2, 3, 4, 5, 6, 7, 8, 9, 10, 11, 12, 13, 14, 15, 16, 17, 18, 19, 20, 21, 22, 23, 24, 25, 26] is of general interest, in particular, in studies of the QCD phase structure [9, 10, 14, 15, 17, 18, 19, 20, 21, 22, 23] and applications in the astrophysics of compact stars [18, 27]. Observable consequences are expected for, e. g., the cooling behavior [28, 29]. Different aspects have been investigated so far, whereby models of the NJL type have been widely employed [30, 31, 32, 33] in studies of the phase structure in the vicinity of the hadronization transition.

Recently, it has been shown in these investigations that for low temperatures (T) and not too large chemical potentials (μ) the two-Flavor Color Superconductivity (2SC) phase is favored over alternative color superconducting phases [20, 21, 24, 25]. According to [25], the Color-Flavor-Locked (CFL) phase occurs only at $\mu \gtrsim 430$ MeV.

It is generally agreed that at low temperatures the transition of the matter from the phase with broken chiral symmetry to the color superconducting phase is of the first order (see e. g. [14]). From the point of view of phenomenological applications, as e.g. in compact star physics, the order of the phase transition to quark superconducting matter plays an important role. The conclusion about the first order phase transition was drawn within models without vector interaction channels taken into account; the vector interaction has been considered in few papers [34, 35]. It was found that the presence of quark interaction in the vector channel moves the critical line in the $\mu - T$ plain to larger μ [14, 36, 37]. Recently it has been demonstrated [38] that the critical line of first order phase transition in the $\mu - T$ plane can have a second end-point at low temperatures, besides the well known one at high temperatures. The latter one could even be subject to experimental verification in heavy-ion collisions [8] whereas the former could be of relevance for neutron stars. While in Ref. [38] this feature of the phase diagram was a consequence of the presence of interaction in the vector channel, we would like to investigate in the present work the sensitivity of the phase diagram to the choice of model parameters without interaction in the vector channel. We will demonstrate that in the absence of the vector channel interaction the phase transition is not necessarily of the first order, thus revising statements in Refs. [37, 39].

It is worth noting that some progress has recently been done in lattice calculations. There are methods being developed that allow to extend lattice

results to the case of finite chemical potentials [40, 41, 42]. However, these methods are valid only for small chemical potentials (see e. g. [40]), below the conditions at which the color superconductivity phase is expected to form.

The structure of our paper is as follows. In Sect. 2, a chiral quark model is introduced, its Lagrangian is given and the model parameters are fixed from the vacuum state in two different schemes. Temperature and chemical potential are introduced into the quark model in Sect. 3, using the Matsubara formalism. The conclusions and a discussion of the obtained results are given in Sect. 4.

2 NJL model with the scalar diquark channel

In order to study the quark matter phase diagram including color superconductivity, one should generalize the concept of the single order parameter related to the quark-antiquark condensate in the case of chiral symmetry breaking to a set of order parameters when condensation can occur in other interaction channels too. The simplest extension is the scalar diquark condensate $\langle \psi\psi \rangle$ for u and d quarks

$$\delta = \langle \bar{\psi} i\gamma_5 \tau_2 \lambda_2 C \bar{\psi}^T \rangle, \quad (1)$$

which is an order parameter characterizing the domain where the color symmetry is spontaneously broken and the quark matter finds itself in the (two-flavor) color superconducting (2SC) state. This quantity is the most important one among other possible condensates that can be constructed in accordance with the Pauli principle [25]. In (1) the matrix C is the charge conjugation matrix operator for fermions

$$C = i\gamma_0\gamma_2. \quad (2)$$

The matrices τ_2 and λ_2 are Pauli and Gell-Mann matrices, respectively. The first one acts on the flavor indices of spinors while the second one acts in the color space.

If the electroweak interaction is discarded and only the strong coupling is in focus, the resulting quark matter phase diagram is essentially determined by nonperturbative features of the QCD vacuum state. One therefore has to resort to nonperturbative approaches to describe the behavior of particles at various conditions, ranging from cold and dilute matter up to the

hot and dense one. A reliable and widely tested model to nonperturbative strong coupling QCD is provided by the Dyson-Schwinger equations [43], however, for qualitative studies like the one we attempt here it proves to be too complex. Therefore, we will use here a simple and tractable nonperturbative model of quark interaction, the Nambu–Jona-Lasinio (NJL) model [30, 31, 32, 33, 44, 45], which has been extensively exploited for the description of the properties of the light meson sector of QCD (also to describe the color superconductivity phase [20, 46, 47]) and proved to be a model respecting the low-energy theorems. Before we proceed to the case of finite temperature and density, the model parameters that determine the quark interaction should be fixed. This shall be done for the vacuum state where hadronic properties are known. We will assume, according to common wisdom that, once fixed, these parameters (originating from the nonperturbative gluon sector of QCD) will not change, even in the vicinity of the transition to the quark matter. This transition is thus caused by medium effects in the quark sector only.

2.1 Lagrangian

In the present paper we restrict ourselves to the two-flavor case, leaving the strange quark and effects related to it beyond our consideration. As we constrain ourselves to only two order parameters, the quark and scalar diquark condensates, during our investigation, the interaction of quarks will be represented in the Lagrangian by $SU(2)_L \times SU(2)_R$ symmetric scalar, pseudoscalar quark-antiquark, and scalar diquark vertices:

$$\mathcal{L} = \bar{\psi}(i\rlap{\not{\partial}} - \hat{m}^0)\psi + \mathcal{L}_{q\bar{q}} + \mathcal{L}_{qq}, \quad (3)$$

$$\mathcal{L}_{q\bar{q}} = \frac{G}{2} [(\bar{\psi}\psi)^2 + (\bar{\psi}i\gamma_5\vec{\tau}\psi)^2], \quad (4)$$

$$\mathcal{L}_{qq} = \frac{H}{2} (\bar{\psi}i\gamma_5\tau_2\lambda_2 C\bar{\psi}^T)(\psi^T C i\gamma_5\tau_2\lambda_2\psi), \quad (5)$$

where \hat{m}^0 is the diagonal current quark mass matrix $\hat{m}^0 = \text{diag}(m_u, m_d)$, G and H are constants describing the interaction of quarks in the scalar, pseudoscalar, and scalar diquark channels, respectively. We work in the isospin symmetric case ($m_u^0 = m_d^0 \equiv m^0$), thus $\hat{m}^0 = m^0 \mathbf{1}_f$.

By the standard Hubbard-Stratonovich procedure, we introduce auxiliary scalar (σ), pseudoscalar triplet ($\vec{\pi}$), and diquark (Δ, Δ^*) fields together

with Yukawa-like terms in the Lagrangian density instead of the four-quark vertices:

$$\begin{aligned} \tilde{\mathcal{L}} = & \bar{\psi}(i \not{\partial} - m^0 + \sigma + i\gamma_5 \vec{\tau} \vec{\pi})\psi - \\ & - \frac{1}{2} \Delta^* \psi^T C \gamma_5 \tau_2 \lambda_2 \psi + \frac{1}{2} \Delta \bar{\psi} \gamma_5 \tau_2 \lambda_2 C \bar{\psi}^T \\ & - \frac{\sigma^2 + \vec{\pi}^2}{2G} - \frac{|\Delta|^2}{2H}. \end{aligned} \quad (6)$$

In order to integrate out the quark degrees of freedom by Gaussian path integration, it is appropriate to represent the quark fields by the bispinor

$$q(x) = \begin{pmatrix} \psi(x) \\ C \bar{\psi}^T(x) \end{pmatrix}, \quad (7)$$

and to introduce the matrix propagator $S(p)$:

$$S^{-1}(p) = \begin{pmatrix} \not{p} - \hat{M} & \Delta \gamma_5 \tau_2 \lambda_2 \\ -\Delta^* \gamma_5 \tau_2 \lambda_2 & \not{p} - \hat{M} \end{pmatrix}. \quad (8)$$

Integrating over $q(x)$ and $\bar{q}(x)$, we then obtain an effective Lagrangian in terms of collective scalar and pseudoscalar quark-antiquark and scalar diquark excitations. Here, we restrict ourselves to the mean-field approximation, leaving the next-to-leading order corrections in the $1/N_c$ expansion beyond our model. Finally, the effective Lagrangian density reads

$$\mathcal{L}_{\text{eff}} = -\frac{\sigma^2 + \vec{\pi}^2}{2G} - \frac{|\Delta|^2}{2H} - i \int \frac{d^4 p}{(2\pi)^4} \frac{1}{2} \text{Tr} \ln (S^{-1}(p)). \quad (9)$$

The trace in (8) is taken in the Dirac, color, and flavor space. The matrix \hat{M} contains σ and $\vec{\pi}$ fields:

$$\hat{M} = (m^0 - \sigma) \mathbf{1} - i\gamma_5 \tau_a \pi_a, \quad (10)$$

the sum over $a = 1, 2, 3$ is assumed, and $\mathbf{1} = \mathbf{1}_c \cdot \mathbf{1}_f \cdot \mathbf{1}_D$.

As it was mentioned above, we are working in the mean-field approximation and the quark condensates are of interest. Therefore, further study can be performed in terms of the effective potential

$$V_{\text{eff}} = - \lim_{v_4 \rightarrow \infty} \frac{1}{v_4} \int_{v_4} d^4 x \mathcal{L}_{\text{eff}} \quad (11)$$

where v_4 is 4-dimensional volume. The vacuum expectation values of the collective variables σ , $\vec{\pi}$, Δ , and Δ^* determine the absolute minimum of V_{eff} . They are given by the equation

$$\frac{\partial V_{\text{eff}}}{\partial \sigma} = \frac{\partial V_{\text{eff}}}{\partial \Delta} = \frac{\partial V_{\text{eff}}}{\partial \Delta^*} = 0 . \quad (12)$$

A priori it is known that in the vacuum only the σ field acquires a nonvanishing expectation value. The diquark fields Δ , Δ^* are expected to have nonzero mean values only in dense matter. The mean value of the pseudoscalar isotriplet field $\vec{\pi}$ is always equal to zero, therefore we omit it hereafter.

Having solved Eq. (12) for the field σ , one can work in terms of the constituent quark mass m , connected with the current quark mass by the gap equation

$$m_0 - m = \langle \sigma \rangle = 2G \langle \bar{\psi} \psi \rangle . \quad (13)$$

In the chiral limit ($m^0 = 0$), the constituent quark mass is proportional to the quark condensate and thus can be treated as the order parameter.

In the NJL model the quark condensate is

$$\langle \bar{\psi} \psi \rangle = -4m I_1^\Lambda(m), \quad (14)$$

where

$$I_1^\Lambda(m) = \frac{-iN_c}{(2\pi)^4} \int \theta(\Lambda^2 - \vec{p}^2) \frac{d^4 p}{m^2 - p^2} . \quad (15)$$

The divergence in $I_1^\Lambda(m)$ is eliminated by means of a sharp 3D cut-off at the scale Λ .

2.2 Parameter fixing

In our model we have four parameters: the four-quark interaction constants G and H , cut-off Λ , and the current quark mass m^0 . Without diquarks, there are only three: G , Λ , and m^0 . They are fixed by the following relations:

1. The Goldberger-Treiman relation (GTR):

$$m = g_\pi F_\pi , \quad (16)$$

where $F_\pi^{\text{exp}} \approx 93$ MeV is the pion weak coupling constant and g_π describes the coupling of a pion with quarks $g_\pi \vec{\pi} \bar{\psi} \vec{\tau} \psi$

$$g_\pi^{-2} = 4I_2^\Lambda(m), \quad I_2^\Lambda(m) = \frac{-iN_c}{(2\pi)^2} \int \frac{\theta(\Lambda^2 - \vec{p}^2) d^4 p}{(m^2 - p^2)^2} . \quad (17)$$

2-a. The quark condensate (QC) from QCD sum rules

$$\langle \bar{\psi}\psi \rangle_{\text{QCDSR}} = -4mI_1^\Lambda(m) \approx (-240 \text{ MeV})^3. \quad (18)$$

2-b. The decay constant g_ρ for the $\rho \rightarrow 2\pi$ (R2PD) process

$$g_\rho = \sqrt{6}g_\pi, \quad g_\rho^{\text{exp}} \approx 6.1. \quad (19)$$

The $\pi - a_1$ transitions are omitted here.

3. The current quark mass m^0 is fixed from the GMOR relation:

$$M_\pi^2 = \frac{-2m^0 \langle \bar{\psi}\psi \rangle}{F_\pi^2}, \quad M_\pi^{\text{exp}} \approx 140 \text{ MeV}. \quad (20)$$

In the chiral limit $M_\pi = 0$, $m^0 = 0$.

4. With the diquark channel included, there is an additional parameter H which can be fixed as $H = 3/4G$ from the Fierz transformation (as e. g. in[20])¹.

In the item 2, we have given two alternatives: one can either use the value of the quark condensate taken from QCD sum rule estimates or demand from the model that it should describe the $\rho \rightarrow 2\pi$ decay. The latter is well observable in experiment contrary to the quark condensate.

For simplicity, we perform all calculations in the chiral limit $m^0 = 0$. In this case, when investigating the hot and dense quark matter, the borders between phases turn out to be sharp and the critical temperature and chemical potential are well defined. With the finite current quark mass, the transitions from one phase to the other become smooth.

As a result, one obtains two different parameter sets shown in Table 1.

In the Type I parameter set the interaction of quarks is stronger, the UV cut-off is smaller, and the constituent quark mass is greater. One can calculate the dimensionless constant $G\Lambda^2$. It equals 4.6 for the Type I and 3.72 for the Type II, respectively. As we will see further, these two parametrizations result in qualitatively different phase diagrams.

¹Some authors use $H = 1/2G$. It turned out that within our model the resulting phase diagram is not much affected if one makes the choice in favor of $H = 1/2G$. However, it would be preferable to fix the constant H from some observable, e. g. from the nucleon mass.

3 NJL model at finite T and μ

3.1 Thermodynamical potential

We extend the NJL model to the case of finite temperatures T and chemical potentials μ , applying the Matsubara formalism, and restrict ourselves to the isospin symmetric case where up and down quark chemical potentials coincide. The thermodynamical potential per volume is

$$\begin{aligned} \Omega(T, \mu) &= -T \sum_n \int \frac{d^3p}{(2\pi)^3} \frac{1}{2} \text{Tr} \ln \left(\frac{1}{T} \tilde{S}^{-1}(i\omega_n, \vec{p}) \right) \\ &+ \frac{\sigma^2}{2G} + \frac{|\Delta|^2}{2H}, \end{aligned} \quad (21)$$

where $\omega_n = (2n + 1)\pi T$ are Matsubara frequencies for fermions, and the chemical potential is included into the definition of inverse quark propagator

$$\tilde{S}^{-1}(p_0, \vec{p}) = \begin{pmatrix} \not{p} - \hat{M} - \mu\gamma_0 & \Delta\gamma_5\tau_2\lambda_2 \\ -\Delta^*\gamma_5\tau_2\lambda_2 & \not{p} - \hat{M} + \mu\gamma_0 \end{pmatrix}. \quad (22)$$

The expression in (21) can be simplified using the equations

$$\begin{aligned} \frac{1}{2} \text{Tr} \ln \left(\tilde{S}^{-1}(i\omega_n, \vec{p}) \right) &= 4 \left[\ln \left(\frac{(\omega_n^2 + E^{+2})(\omega_n^2 + E^{-2})}{T^4} \right) \right] \\ &+ 2 \left[\ln \left(\frac{(\omega_n^2 + \epsilon^{+2})(\omega_n^2 + \epsilon^{-2})}{T^4} \right) \right] \end{aligned} \quad (23)$$

and

$$T \sum_{n=-\infty}^{\infty} \ln \left(\frac{(\omega_n^2 + E^{\pm 2})}{T^2} \right) = E^{\pm} + 2T \ln[1 + \exp(-E^{\pm}/T)]. \quad (24)$$

$$\begin{aligned} \Omega(T, \mu) &= - \int \frac{d^3p}{(2\pi)^3} \left\{ 2 \left(2\epsilon\theta(\Lambda^2 - \vec{p}^2) + 2T \ln \left[1 + \exp \left(-\frac{\epsilon^+}{T} \right) \right] \right. \right. \\ &+ \left. \left. 2T \ln \left[1 + \exp \left(-\frac{\epsilon^-}{T} \right) \right] \right) \right. \\ &+ \left. 4 \left((E^+ + E^-) \theta(\Lambda^2 - \vec{p}^2) + 2T \ln \left[1 + \exp \left(-\frac{E^+}{T} \right) \right] \right. \right. \\ &+ \left. \left. 2T \ln \left[1 + \exp \left(-\frac{E^-}{T} \right) \right] \right) \right\} + \frac{m^2}{2G} + \frac{|\Delta|^2}{2H}, \end{aligned} \quad (25)$$

where

$$\epsilon = \sqrt{\vec{p}^2 + m^2}, \quad \epsilon^\pm = \epsilon \pm \mu, \quad (26)$$

$$E^\pm = \sqrt{(\epsilon^\pm)^2 + |\Delta|^2}. \quad (27)$$

The cold matter limit $T = 0$ looks as follows:

$$\begin{aligned} \Omega(0, \mu) &= - \int \frac{d^3p}{(2\pi)^3} [2(|\epsilon^+| + |\epsilon^-|) + 4(E^+ + E^-)] \\ &\times \theta(\Lambda^2 - \vec{p}^2) + \frac{m^2}{2G} + \frac{|\Delta|^2}{2H}. \end{aligned} \quad (28)$$

The thermodynamical potential cannot be calculated in closed form for arbitrary T and μ . However, in the cold matter limit one can easily obtain analytic expressions for the thermodynamical potential or its derivatives if only one of the collective variables σ or $|\Delta|$ has a nonvanishing average value. This allows to find what kind of phase transition is to be expected for different parameter choices.

We evaluate the remaining 3D momentum integrals numerically and calculate the value of thermodynamical potential at different T and μ for the two types of model parameter sets. The equilibrium state for each T and μ is determined by $\langle \sigma \rangle = -m$ and $\langle |\Delta| \rangle$ corresponding to the minimum of $\Omega(T, \mu)$.

3.2 Numerical results: Type I

It is quite illustrative to look at the contour plots of the thermodynamical potential. For several values of μ at $T = 0$ they are shown in Figs. 1–4 where one can follow the appearance and disappearance of local minima, maxima, and saddle points of the thermodynamical potential with increasing chemical potential. For zero temperature and chemical potential we have, as expected, a nonzero constituent quark mass (quark condensate) corresponding to the absolute minimum of the thermodynamical potential at $m \sim 350$ MeV and $\langle |\Delta| \rangle = 0$ in Fig. 1. At a certain chemical potential, a new local minimum related to the diquark condensate near $\langle |\Delta| \rangle \sim 110$ MeV and $m = 0$ (Fig. 2), but it does not yet give the absolute minimum. There is also a local maximum around $m \sim 200$ MeV and $\langle |\Delta| \rangle = 0$. As the matter becomes more dense, the second minimum lowers until it becomes degenerate with the first minimum while the average value of σ (or $-m$) remains almost unchanged

(see Fig. 3). Above the corresponding (critical) chemical potential $\mu_c \approx 321$ MeV, the second minimum becomes the absolute one and a first order transition occurs, during which $\langle\sigma\rangle$ discontinuously changes to zero while the diquark condensate acquires nonzero value breaking the color symmetry of the strong interaction. This characterizes the color superconducting phase transition in quark matter. Furthermore, the local minimum on the m axis merges the saddle point (see Fig. 4) and, at still higher μ , only the local minimum on the Δ axis near $|\Delta| \sim 130$ MeV and $m = 0$ remains.

At a fixed chemical potential above μ_c , with the temperature rising, the average value of $|\Delta|$ decreases until it reaches zero at the critical temperature T_c which can be roughly estimated using the BCS theory formula

$$T_c \approx 0.57 \langle|\Delta|\rangle_{T=0} . \quad (29)$$

Above this temperature quark matter is in the symmetric phase ² where the chiral and color symmetries are restored. Finally, we obtain the phase diagram shown on Fig. 5 with three phases: the hadron phase, 2SC phase, and symmetric phase. All three phases coexist at the triple point: $T_t \approx 55$ MeV and $\mu_t \approx 305$ MeV.

3.3 Numerical results: Type II

As for the Type I parameter set, at zero T and μ only the constituent quark mass m , being the order parameter for the chiral condensate, is nonzero, whereas the diquark gap Δ vanishes. However, the vacuum value of m is lower than that for the Type I and, with the chemical potential increasing, μ becomes equal to the vacuum value of m before the second local minimum, corresponding to the diquark condensate, appears. At further increase of μ the constituent quark mass decreases, and it would vanish at $\mu = \mu_1$,

$$\mu_1 = \sqrt{\Lambda^2 - \frac{\pi^2}{3G}} , \quad (30)$$

if the diquark condensate did not appear. Actually, at the critical value μ_1 both the quark condensate and the diquark condensate are small but nonzero.

The changes of the local extrema for increasing chemical potential are similar to those shown in Figs. 1–4. The cases of dilute ($\mu = 0$) and very

²According to recent investigations [48], a so-called pseudo-gap phase as a precursor of color superconductivity can occur in this region.

dense matter ($\mu = 400$ MeV) are qualitatively analogous, only the absolute values of m and $|\Delta|$ at which the local minima are found are different. At intermediate densities, however, there is a qualitative difference. Within a very narrow range of values of the chemical potential, there exists a new phase of massive superconducting matter. One can see this in Fig. 6 for $\mu = 286$ MeV. At higher μ the chiral symmetry is restored and the quark matter is in the pure superconducting phase. A possibility of the chiral diquark condensates to coexist at certain condition has been already noticed in Ref. [49]

Thus, for the Type II parameter set, the transition from the hadronic to the superconducting phase is of the second order. In this case there are no degenerate local minima in the thermodynamical potential separated by a barrier. This behavior is unlike to what is commonly expected for a cold and dense matter but it parallels the findings of Ref. [38] where vector interactions are responsible for this behavior.

The average value of $|\Delta|$ is much smaller than for the Type I parameter set. As a consequence, the border between 2SC and the symmetric phases of quark matter lies at noticeably lower temperatures. The phase diagram obtained in our model for the Type II parameter set is shown in Fig. 7.

4 Conclusion

In the framework of the simple NJL model for two flavors, a phase diagram is obtained for $T = 0$ –200 MeV and $\mu = 0$ –450 MeV. Three phases are found for the Type I parameter set and four phases for the Type II parameter set. The critical temperature and chemical potential obtained in the Type I scheme differ from those obtained with the Type II parameter set. At $T = 0$, $\mu_c \approx 320$ MeV for the Type I parameter set and $\mu_c \approx 288$ MeV for the Type II. The corresponding quark densities differ by a factor 1.5 – 1.7. The critical temperature for the Type II parameter set is as low as 7 MeV and thus much closer to critical temperatures for the pairing instability in nuclear matter systems (see [50]) whereas for the Type I parameter set the critical temperatures are an order of magnitude larger. This striking difference in the critical parameters obtained within the same model calls for a more detailed investigation of the question of model parametrization.

In our work, the constant H was not obtained from a fit to observable data. Instead, Fierz transformation arguments have been used to fix the

ratio $H/G = 3/4$. A parameterization would be favourable where (in the spirit of the Type II model) experimentally measured quantities, like the ρ meson width, are used rather than non-observable ones (quark condensate etc.). It would therefore be more consistent to fit the constant H from baryon properties, see [51, 52] and also to go beyond the mean field level of description. These investigations shall be performed in future work where it remains to be clarified which critical parameters for the color superconducting phase transition can be considered more realistic and of which order the phase transition is.

Acknowledgement

The authors are grateful to M. Buballa, T. Kunihiro, and M. Kitazawa for useful discussions. This work has been supported by DAAD and Heisenberg-Landau programs. V.Y. and M.K.V. acknowledge support by RFBR grant No. 02-02-16194.

References

- [1] B. Barrois, Nucl. Phys. B **129**, 390 (1977).
- [2] D. Bailin and A. Love, Phys. Rep. **107**, 325 (1984).
- [3] M. Iwasaki and T. Iwado, Phys. Lett. B **350**, 163 (1995).
- [4] M. Iwasaki and T. Iwado, Prog. Theor. Phys. **94**, 1073 (1995).
- [5] M. Alford, K. Rajagopal, and F. Wilczek, Phys. Lett. B **422**, 247 (1998).
- [6] R. Rapp, T. Schäfer, E. V. Shuryak, and M. Velkovsky, Phys. Rev. Lett. **81**, 53 (1998).
- [7] M. A. Halasz, A. D. Jackson, R. E. Shrock, M. A. Stephanov, and J. J. Verbaarschot, Phys. Rev. D **58**, 096007 (1998);
- [8] M. A. Stephanov, K. Rajagopal, and E. V. Shuryak, Phys. Rev. Lett. **81**, 1998 (4816).
- [9] J. C. R. Bloch, C. D. Roberts, and S. M. Schmidt, Phys. Rev. C **60**, 065208 (1999).

- [10] M. Alford, K. Rajagopal, and F. Wilczek, Nucl. Phys. B **573**, 443 (1999).
- [11] R. D. Pisarski and D. H. Rischke, Phys. Rev. Lett. **83**, 37 (1999).
- [12] D. T. Son, Phys. Rev. D **59**, 094019 (1999).
- [13] T. Schäfer and F. Wilczek, Phys. Rev. D **60**, 114033 (1999).
- [14] J. Berges and K. Rajagopal, Nucl. Phys. B **538**, 215 (1999).
- [15] R. Rapp, T. Schäfer, E. V. Shuryak, and M. Velkovsky, Ann. Phys. **280**, 35 (2000).
- [16] R. D. Pisarski and D. H. Rischke, Phys. Rev. D **61**, 051501 (2000).
- [17] K. Rajagopal and F. Wilczek, arXiv: hep-ph/0011333 and references therein, in: Shifman, M. (ed.): *At the frontier of particle physics*, vol. 3, World Scientific, Singapore (2002), pp. 2061–2151.
- [18] M. Alford, Ann. Rev. Nucl. Part. Sci. **51**, 131 (2001).
- [19] M. Alford, K. Rajagopal, S. Reddy, and F. Wilczek, Phys. Rev. D **64**, 074017 (2001).
- [20] M. Buballa and M. Oertel, Nucl. Phys. A **703**, 770 (2002).
- [21] M. Oertel and M. Buballa, in: *Ultrarelativistic heavy-ion collisions*, Proc. Int. Workshop XXX on gross properties of nuclei and nuclear excitations, Hirschegg/Austria, M. Buballa, W. Nörenberg, B.-J. Schäfer, and J. Wambach (Eds.), Darmstadt (2002).
- [22] F. Gastineau, R. Nebauer, and J. Aichelin, Phys. Rev. C **65**, 045204 (2002).
- [23] M. Harada and S. Takagi, Progr. Theor. Phys. **107**, 561 (2002).
- [24] A. Steiner, S. Reddy, and M. Prakash, Phys. Rev. D **66**, 094007 (2002).
- [25] F. Neumann, M. Buballa, and M. Oertel, Nucl. Phys. A **714**, 481 (2003).
- [26] J. Bowers and K. Rajagopal, Phys. Rev. D **66**, 065002 (2002).
- [27] D. Blaschke, N. K. Glendenning, A. Sedrakian (Eds.), *Physics of Neutron Star Interiors*, (Springer, LNP 578, 2001).

- [28] D. Blaschke, T. Klähn, and D. N. Voskresensky, *Astrophys. J.* **533**, 406 (2000).
- [29] D. Blaschke, H. Grigorian, and D. N. Voskresensky, *Astron. & Astrophys.* **368**, 561 (2001).
- [30] D. Ebert and H. Reinhardt, *Nucl. Phys. B* **271**, 188 (1986).
- [31] M. K. Volkov, *Sov. J. Part and Nucl.* **17**, 186 (1986).
- [32] D. Ebert, Yu. L. Kalinovsky, L. Münchow, and M. K. Volkov, *Int. J. Mod. Phys. A* **8**, 1295 (1993).
- [33] D. B. Blaschke, G. R. G. Burau, M. K. Volkov, and V. L. Yudin, *Eur. Phys. J. A* **11**, 319 (2001).
- [34] K. Langfeld and M. Rho, *Nucl. Phys. A* **660**, 475 (1999).
- [35] M. Buballa, J. Hošek, and M. Oertel, *Phys. Rev. D* **65**, 014018 (2001)
- [36] S. Klimt, M. Lutz, and W. Weise, *Phys. Lett. B* **249**, 249 (1990)
- [37] M. Asakawa and K. Yazaki, *Nucl. Phys. A* **504**, 668 (1989).
- [38] M. Kitazawa, T. Koide, T. Kunihiro, and Y. Nemoto, *Prog. Theor. Phys.* **108**, 929 (2002).
- [39] T. Kunihiro, *Nucl. Phys. B* **351**, 593 (1991).
- [40] C. R. Allton, S. Ejiri, S. J. Hands, O. Kaczmarek, F. Karsch, E. Laermann, C. Schmidt, L. Scorzato, *Phys. Rev. D* **66**, 074507 (2002).
- [41] S. D. Katz and Z. Fodor, *JHEP* **0203**, 014 (2002).
- [42] F. Csikor, G. I. Egri, Z. Fodor, S. D. katz, K. K. Szabo, A. I. Toth, hep-lat/0301027.
- [43] C. D. Roberts and S. M. Schmidt, *Prog. Part. Nucl. Phys.* **45** (2000) S1 [arXiv:nucl-th/0005064].
- [44] S. P. Klevansky, *Rev. Mod. Phys.* **64**, 649 (1992).
- [45] T. Hatsuda and T. Kunihiro, *Phys. Rep.* **247**, 221 (1994).

- [46] D. Ebert, Ch. V. Zhukovsky, A. S. Vshivtsev, *Int. J. Mod. Phys. A* **13**, 1723 (1998) *Phys. Rev. C* **61**, 055209 (2000).
- [47] T. M. Schwarz, S. P. Klevansky, and G. Papp, *Phys. Rev. C* **60**, 055205 (1999).
- [48] M. Kitazawa, T. Koide, T. Kunihiro, and Y. Nemoto, *Phys. Rev. D* **65**, 091504 (2002).
- [49] M. Sadzikowski, *Mod. Phys. Lett. A* **16**, 1129 (2001).
- [50] A. Sedrakian and U. Lombardo, *Phys. Rev. Lett.* **84**, 602 (2000) and references therein.
- [51] S. Pepin, M. C. Birse, J. A. McGovern, and N. R. Walet, *Phys. Rev. C* **61**, 055209 (2000).
- [52] W. Bentz, T. Horikawa, N. Ishii, and A. W. Thomas, arXiv:nucl-th/0210067.

Tables

	Λ [GeV]	G [GeV ⁻²]	H [GeV ⁻²]	m [MeV]	$\sqrt[3]{-\langle\bar{\psi}\psi\rangle}$ [MeV]	g_ρ
GTR+QC [Type I]	600	12.8	9.6	350	240	9.2
GTR+R2PD [Type II]	856	5.1	3.8	233	284	6.1

Table 1: The model parameters for two different schemes of parameter fixing. The first row corresponds to the case where the quark condensate value is used, while in the second row the parameters correspond to the case where the decay width of the process $\rho \rightarrow 2\pi$ is used.

Figures

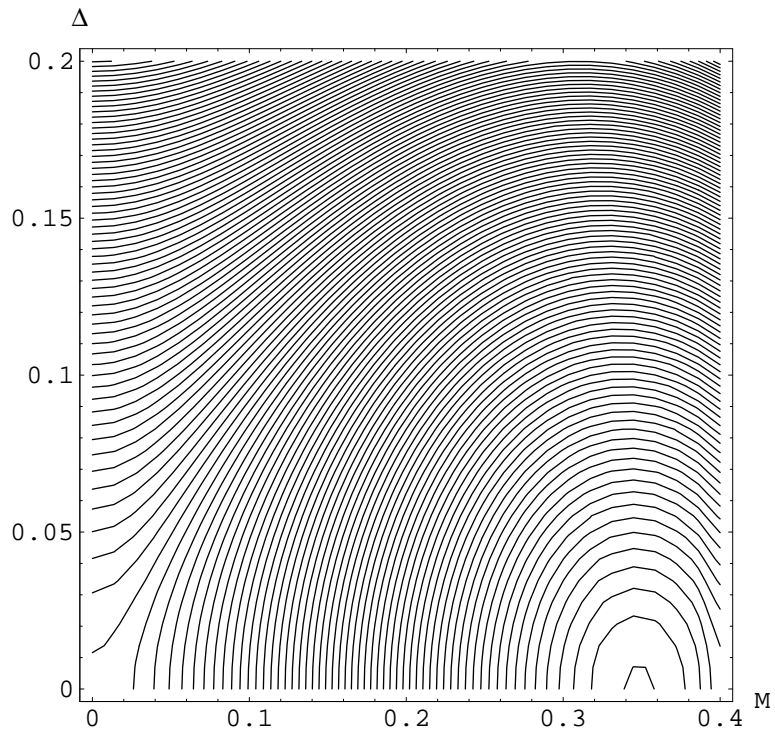


Figure 1: The contour plot for the thermodynamic potential as a function of m and Δ at zero temperature and the chemical potential $\mu = 0$ MeV.

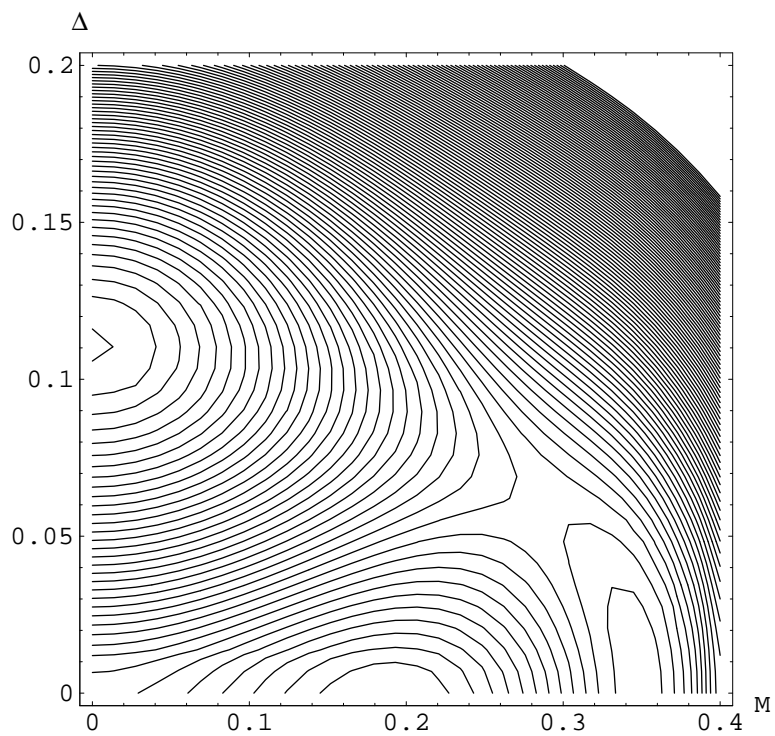


Figure 2: The contour plot for the thermodynamic potential as a function of m and Δ at zero temperature and the chemical potential $\mu = 340$ MeV.

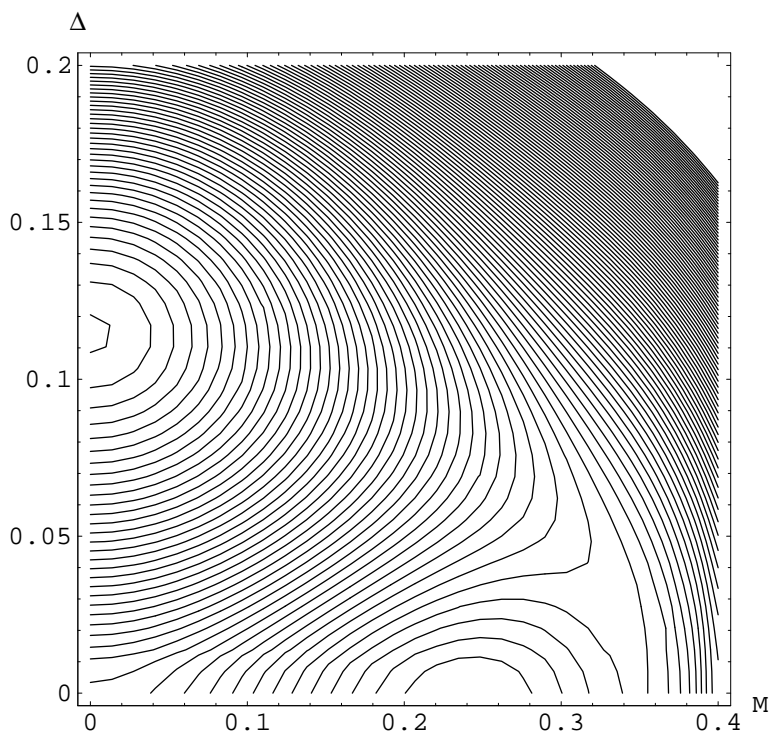


Figure 3: The contour plot for the thermodynamic potential as a function of m and Δ at zero temperature and the chemical potential $\mu = 350$ MeV.

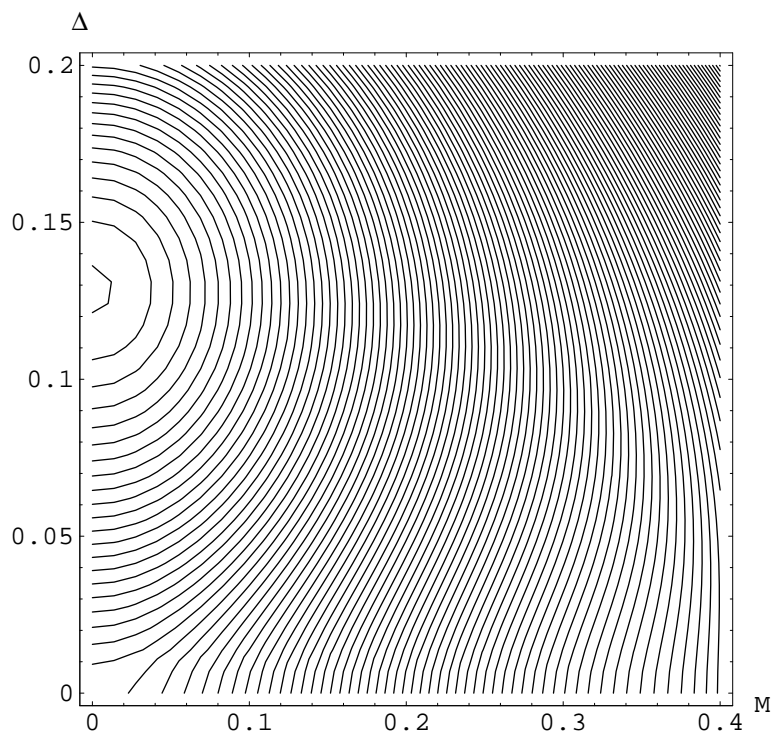


Figure 4: The contour plot for the thermodynamic potential as a function of m and Δ at zero temperature and the chemical potential $\mu = 400$ MeV.

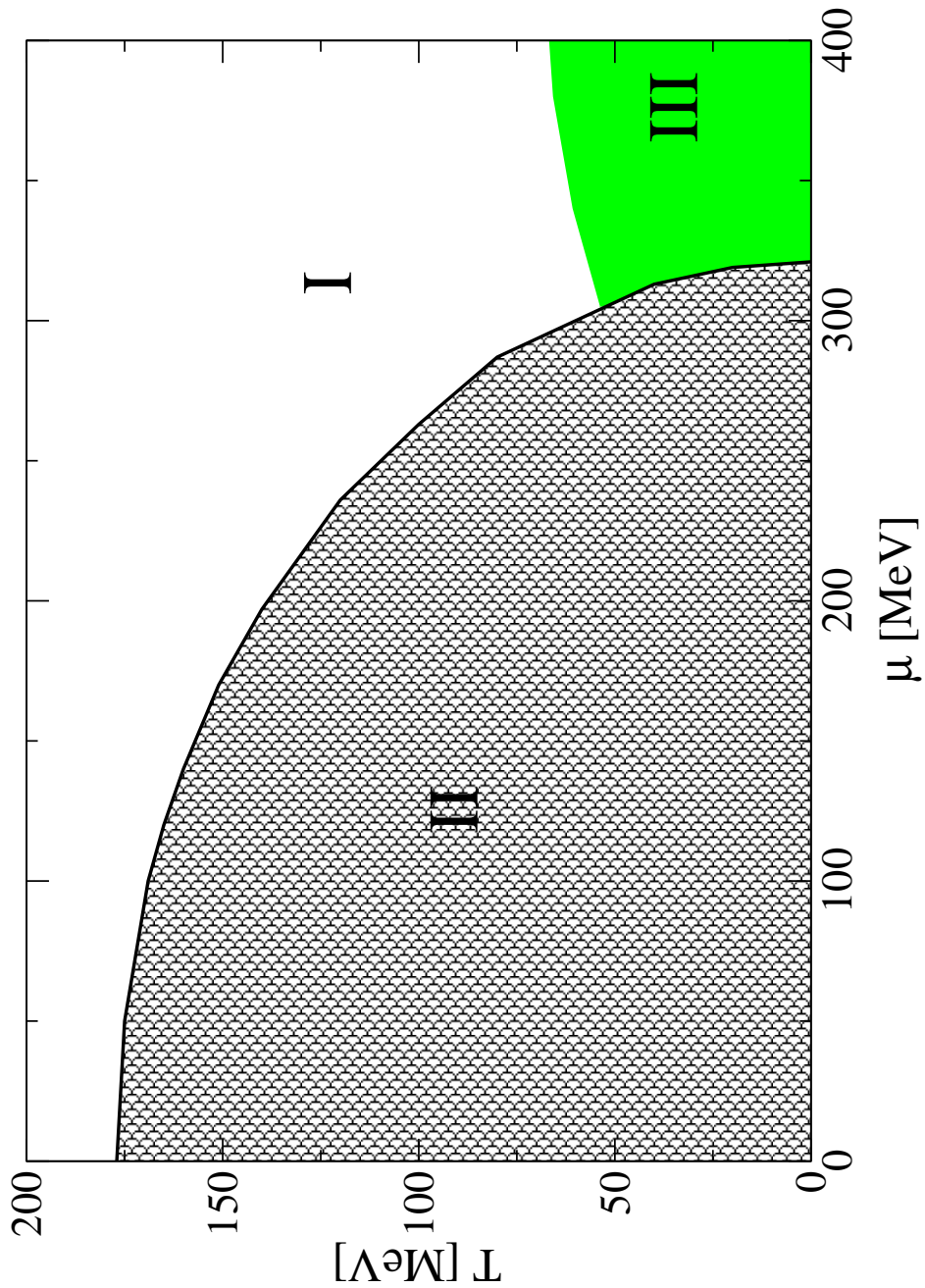


Figure 5: The quark matter phase diagram from the NJL model with the Type I parameter set. In phase I both chiral and diquark condensates vanish; in phase II the chiral symmetry is broken; in phase III the chiral symmetry is restored while the diquark condensate is nonzero.

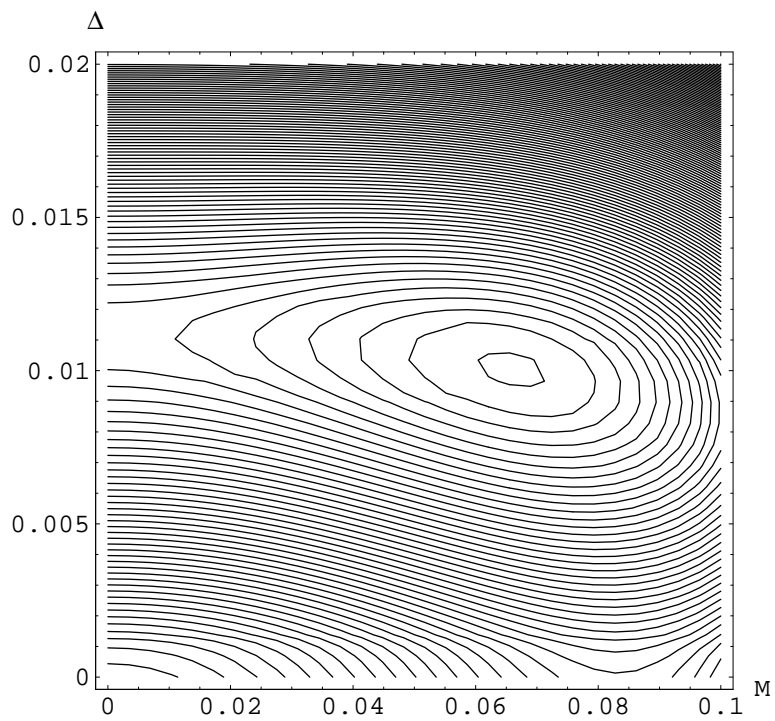


Figure 6: The contour plot for the thermodynamic potential as a function of m and Δ at zero temperature and the chemical potential $\mu = 286$ MeV for the Type II parameter set.

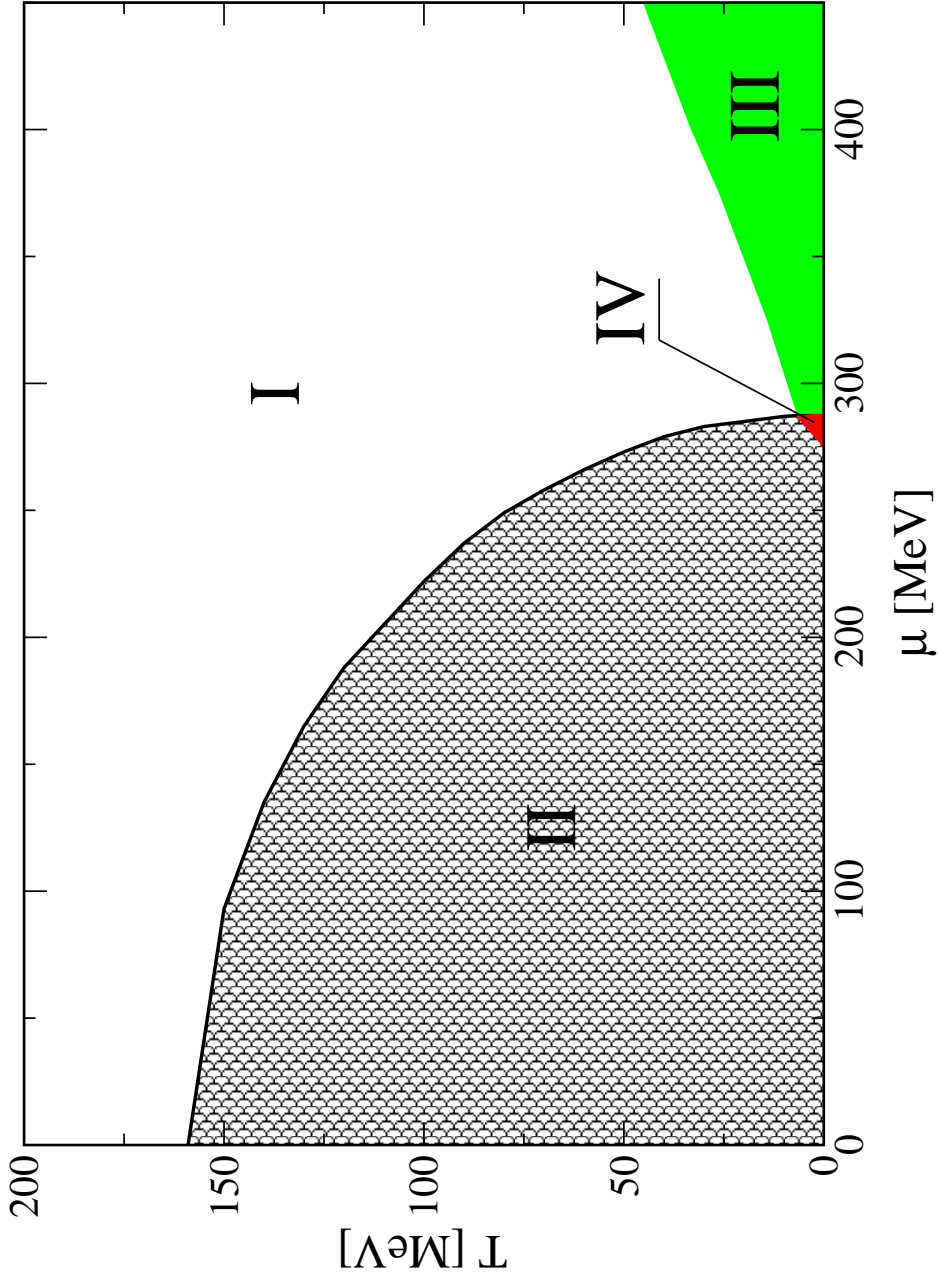


Figure 7: The quark matter phase diagram from the NJL model with the Type II parameter set. In phase I both chiral and diquark condensates vanish; in phase II the chiral symmetry is broken; in phase III the chiral symmetry is restored while the diquark condensate is nonzero; in phase IV both the chiral and diquark condensates coexist.